Title
Cleaving Off Uranyl Oxygens through Chelation: A Mechanistic Study in the Gas Phase

Journal
Inorganic Chemistry, 56(21)

ISSN
0020-1669

Authors
Abergel, Rebecca J
de Jong, Wibe A
Deblonde, Gauthier J-P
et al.

Publication Date
2017-11-06

DOI
10.1021/acs.inorgchem.7b01720

Peer reviewed

Cleaving Off Uranyl Oxygens through Chelation: A Mechanistic Study in the Gas Phase

*Rebecca J. Abergel[*1], Wibe A. de Jong[*2], Gauthier J-P. Deblonde[1], Phuong D. Dau[1], Ilya Captain[1], Teresa M. Eaton[1], Jiwen Jian[1], Michael J. van Stipdonk[3], Jonathan Martens[4], Giel Berden[4], Jos Oomens[4,5], and John K. Gibson[*1].*

[1]Chemical Sciences Division, Lawrence Berkeley National Laboratory, Berkeley, California 94720, USA

[2]Computational Research Division, Lawrence Berkeley National Laboratory, Berkeley, California 94720, USA

[3]Department of Chemistry and Biochemistry, Duquesne University, Pittsburgh, Pennsylvania 15282, USA

[4]Radboud University, Institute for Molecules and Materials, FELIX Laboratory, Toernooiveld 7c, 6525ED Nijmegen, The Netherlands

[5]Van‘t Hoff Institute for Molecular Sciences, University of Amsterdam, Science Park 904, 1098XH Amsterdam, The Netherlands

ABSTRACT

Recent efforts to activate the strong uranium-oxygen bonds in the dioxo uranyl cation have been limited to single oxo-group activation through either uranyl reduction and functionalization in solution, or by collision induced dissociation (CID) in the gas-phase, using mass spectrometry (MS). Here we report and investigate the surprising double activation of uranyl by an organic ligand, 3,4,3-LI(CAM), leading to the formation of a formal U^{6+} chelate in the gas-phase. The cleavage of both uranyl oxo bonds was experimentally evidenced by CID, using deuterium and ^{18}O isotopic substitutions, and by infrared multiple photon dissociation (IRMPD) spectroscopy. Density functional theory (DFT) computations predict that the overall reaction requires only 132 kJ/mol, with the first oxygen activation entailing about 107 kJ/mol. Combined with analysis of similar, but unreactive ligands, these results shed light on the chelation-driven mechanism of uranyl oxo bond cleavage, demonstrating its dependence on the presence of ligand hydroxyl protons available for direct interactions with the uranyl oxygens.

KEYWORDS Uranyl activation, Actinide chemistry, Gas-phase chemistry, Collision induced dissociation, Uranium chelate

INTRODUCTION

Ubiquitous in current nuclear fuel cycle operations and in future recovery processes of U from seawater, the uranyl ion, UO_2^{2+}, occupies a central place in the nuclear chemistry field.[1–5] In spite of its apparent chemical inertness, UO_2^{2+} has recently caught growing attention for the tantalizing prospect of activating its remarkably stable metal-oxygen double bonds.[6] Nevertheless, the activation and functionalization of UO_2^{2+} still remain challenging and elusive. In the condensed phase, a few examples of apparent activation and functionalization of the highly stable U=O bonds have been proposed recently, with notably the reductive silylation and coordination by a Lewis acid such as $B(C_6F_5)_3$ or an alkali metal.[7–9] However, with these approaches, the uranyl oxo bond (U=O) undergoes reduction due to the instability of the hypothetical UO^{4+} or U^{6+} ions. In the gas-phase, three mono-activated UO_2^{2+} systems have been prepared recently by CID-MS experiments. Upon CID,[10] the $[UO_2(N_3)Cl_2]^-$ complex dissociated into the activated $[UO(NO)Cl_2]^-$ ion via N_2 loss. $[UO_2(NCO)Cl_2]^-$ was obtained similarly[11] by electrospray ionization (ESI), with subsequent CID yielding the elimination of CO_2 and the direct formation of the oxo-nitride $[UONCl_2]^-$. Likewise, the UON^+ complex was prepared from $[UO_2(NC)]^+$.[12] For each of the UON^+, $[UO(NO)Cl_2]^-$ and $[UONCl_2]^-$ systems, only one of the UO_2^{2+} oxo bonds was cleaved and replaced by another inorganic ligand, resulting in a sequence of compounds in which the metal center keeps its +VI oxidation state. Only one previous report describes the substitution of both U=O bonds and the formation of a U(VI) aryloxide, as the result of $[HNC_5H_5]_2[UO_2Cl_4]$ complexation with ^{t}Bu-calix[6]arene and $La(OTf)_3$.[13] While characterization of this reaction's product revealed an octahedral U(VI) atom ligated by three phenolate oxygens from each of two calixarene ligands, the mechanism of activation was not understood.[13,14] Drawing from this report and from previously performed gas-phase mono-activation reactions,

we sought to investigate potential mechanisms associated with the cleavage of both UO_2^{2+} oxo bonds, using chelated UO_2^{2+} as a starting reagent. Here, we describe the non-reductive UO_2^{2+} oxo activation by an octadentate catecholamide ligand, 3,4,3-LI(CAM), leading to the cleavage of both U=O bonds and the formation of a formal U^{6+} chelate in the gas-phase. Through a combination of spectroscopic and computational tools, interactions between the ligand and metal center were probed and helped deciphering the activation mechanism to provide a rationale for the design of new synthetic systems with uranyl-oxo functionalization properties.

METHODS

Caution! *Uranium compounds are hazardous and radioactive materials that should only be manipulated in specifically designated facilities in accordance with appropriate safety controls.*

Chemicals

The ligands 3,4,3-LI(1,2-HOPO)[15] ($HOPOH_6$) and 3,4,3-LI-CAM[16] ($CAMH_{10}$) were synthesized and characterized as previously reported. Ligand stock solutions were prepared by direct dissolution in DMSO. Deuterium-substituted $CAMD_{10}$ was prepared by facile exchange of the eight hydroxyl and two amide hydrogen atoms with the deuterium atoms upon dissolution of the ligand in D_2O; exchange was confirmed by the 7 m/z shift relative to $[UO_2(CAMH_7)]^-$. Aqueous stock solutions of natural uranyl were prepared from UO_2Cl_2. An 18.6 mM stock solution of ^{18}O-labeled uranyl was prepared by dissolution of UO_2Cl_2 in $H_2{}^{18}O$ (Sigma Aldrich, 97% ^{18}O), followed by UV irradiation for 90 hours. Uranyl concentration was determined by UV-vis spectrophotometry using an ε(414 nm) value of 9.7 $L.mol^{-1}.cm^{-1}$,[17] and the oxygen exchange in the UO_2Cl_2 stock was confirmed by ESI-MS.

ESI-MS Experiments

The general experimental approach has been described previously.[18,19] Anionic complexes of uranyl and triply de-protonated ligands were produced by ESI of ethanol solutions (~80% ethanol; 20% water) containing 100 μM $UO_2Cl_2^-$ (diluted from 10 mM UO_2Cl_2 at pH = 2) and 100 μM of the chelating ligand. The experiments were performed using an Agilent 6340 quadrupole ion trap mass spectrometer with MS^n CID capability; the CID energy is an instrumental parameter that provides only a relative indication of ion excitation. Anion mass spectra were acquired using the following parameters: solution flow rate, 60 μL.h^{-1}; nebulizer gas pressure, 12 psi; capillary voltage offset and current, -4000 V and 24.5 nA; end plate voltage offset and current, -500 V and 3025.0 nA; dry gas flow rate, 3 L.min^{-1}; dry gas temperature, 325°C; capillary exit, -50.0 V; skimmer, -36.3 V; octopole 1 and 2 DC, -10.88 V and -3.00 V; octopole RF amplitude, 190 Vpp; lens 1 and 2, 10.0 V and 91.0 V; trap drive, 50.0. Nitrogen gas for nebulization and drying was supplied from the boil-off of a liquid nitrogen Dewar. The background water pressure in the ion trap is estimated as ~10^{-6} Torr and reproducibility of hydration rates of $UO_2(OH)^+$ established that the water pressure was constant to within <10%.[20] The helium buffer gas pressure in the trap is constant at ~10^{-4} Torr.

IRMPD Experiments

The IRMPD experiments were performed at the Free Electron Laser for Infrared eXperiments (FELIX) Laboratory.[21] The $[UO_2(CAMH_7)]^-$ and $[UO_2(HOPOH_3)]^-$ complexes were produced by ESI of similar solutions and under similar conditions as employed for the gas-phase reactivity studies described above, with subsequent CID to induce water loss from the former. The IRMPD spectra were acquired using a QIT/MS similar to that previously employed to study uranyl-

crown and organouranyl complexes.[22,23] The QIT/MS has been modified[24,25] such that the high-intensity tunable IR beam from FELIX can be directed onto the ion packet, resulting in multiphoton dissociation that is appreciable only when the IR frequency is resonant with a sufficiently intense absorption vibrational mode of the particular mass-selected complex being studied. The FEL produces ~5 μs long IR pulses with an energy of ~40 mJ/pulse at a repetition rate of 10 Hz. For the IRMPD measurements described here, ions were irradiated for 200 ms, corresponding to two FEL pulses, before being scanned out of the trap and detected.

Computational Simulations

Density functional theory calculations were performed with the open-source NWChem software suite.[26] The Stuttgart small-core effective core-potential and associated basis set[27] were used to describe the uranium atom, while all-electron DFT optimized valence triple-ζ polarized (TZVP) basis sets[28] were used for all other atoms in the modeled complexes. The geometries of the complexes were optimized, followed by frequency calculations to ensure the calculated structure had no imaginary frequencies and was in a minimum energy configuration. To validate the computational approach, additional geometry optimizations with and all-electron DFT optimized valence triple-ζ polarized (TZVP) basis sets on the light elements were done. All reaction energies obtained from the calculations include the zero-point energy correction. The vibrational frequencies were scaled empirically with a factor 0.985 and subsequently converted into an infrared spectrum by applying a Gaussian broadening (10 cm^{-1} full width at half maximum) to each mode utilizing the calculated intensities and summing all broadened peaks to form the final spectrum.

RESULTS AND DISCUSSION

Samples containing an equimolar amount of UO_2Cl_2 and the catecholamide siderophore derivative 3,4,3-LI(CAM) (Fig. **1**, hereafter designated as $CAMH_{10}$ to denote the hydroxyl and amide H atoms) in ethanol were subjected to ESI, resulting in the formation of the gas-phase 1:1 chelate $[UO_2(CAMH_7)]^-$. Similar experiments performed with the deuterated analogue $CAMD_{10}$, where the labile catechol and secondary amide protons have been exchanged with deuterium to yield the deuterated chelate $[UO_2(CAMD_7)]^-$. Both complexes (m/z = 1113, or 1120 when deuterated) were selected from their parent ESI mass spectra and subjected to CID, which resulted primarily in the loss of two water molecules, as depicted in Figure **1**. The dissociation pattern was similar for the hydrogen and deuterium versions of the system indicating that the four labile protons are removed from the ligand upon elimination of the two water molecules. Based on these results, the eliminated oxygen atoms present in H_2O and D_2O could be from either the ligand or the metal dioxo cation.

Aside from the loss of the water molecules, whether deuterated or protonated, the complex also dissociates by losing one binding unit due to the cleavage of one of its two secondary amide C-N bonds. The mass of the resulting fragmented species (m/z = 877) corresponds to a mono-charged complex comprising the 3 remaining catechol units, the spermine backbone of the ligand with a primary amine due to the H-transfer from the eliminated sub-fragment (m/z = 136), and a UO_2^{2+} ion.

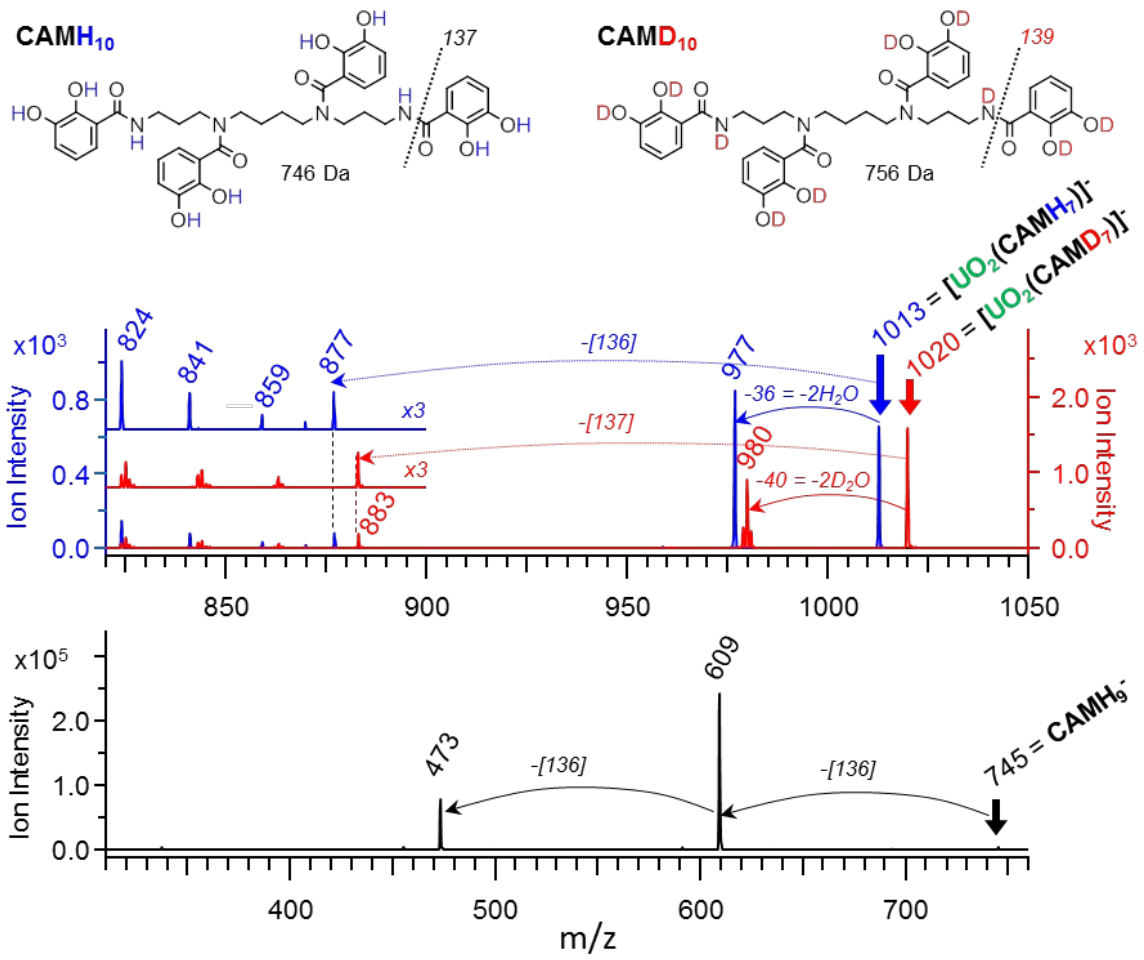

Figure 1. (top) CID ESI-MS spectra of $[UO_2(CAMH_7)]^-$ (blue) and $[UO_2(CAMD_7)]^-$ (red). Nominal CID voltage = 0.25 V. (bottom) CID ESI-MS spectrum of the ligand $CAMH_9^-$. Nominal CID voltage = 0.70 V. The structures of the ligand ($CAMH_{10}$) and its deuterated version ($CAMD_{10}$) are given for clarity. The dominant fragmentation pathways are two H_2O losses for $[UO_2(CAMH_7)]^-$ and two D_2O losses for $[UO_2(CAMD_7)]^-$; water loss is not observed for $CAMH_9^-$. Also observed are ligand cleavages as indicated, concomitant with H-atom transfer from the eliminated neutral fragment (136 m/z); this is the only pathway observed for the ligand. Although the fragmentation mechanisms are not revealed by these results, the peaks at 859, 841, and 824 m/z correspond to the respective losses of "136" and one H_2O; "136" and two H_2O; and "136", two H_2O, and one OH from $[UO_2(CAMH_7)]^-$.

The elimination pathway was similar to that observed with the deuterated complex. Formation of three additional species was observed, corresponding to the combined loss of this sub-fragment with one (m/z 859) or two (m/z 841) water molecules, and further elimination of an OH

group (m/z 824). This OH elimination was not observed after the direct departure of the two water molecules from the parent ion as shown by the absence of ion intensity at m/z 960 and 962 (Fig. **1**). It is apparent that the additional fragmentation pathways are not a result of simple loss of a ligand fragment from the dominant double-water-loss pathway of primary interest here. Of note, CID of the deprotonated ligand $CAMH_9^-$, in the absence of uranyl, resulted in two consecutive eliminations of m/z 136 only, corresponding to the sequential departure of two catechol units, strongly indicating that the water losses were indeed induced by the actinyl ion and did not arise from the CAM ligand itself.

DFT calculations were performed to gain insights into the oxygen source of the water dissociation chemistry of $[UO_2(CAMH_7)]^-$. The calculated lowest energy structures for the product, intermediate (single water loss) and reactant complexes are shown in Figure **2** and Supplementary Figure **S1**. Uranyl U=O bond lengths in $[UO_2(CAMH_7)]^-$ (Fig. **2**, left panel) are 1.80 and 1.81 Å while the uranyl is almost linear with a 178-degree O-U-O angle. Protons from two catechol units are oriented towards the uranyl oxygens, at distances of 1.88 and 1.98 Å from the oxygen with a third available proton at a larger distance (2.78 Å). Four oxygens from the remaining catechol units are located approximately in the equatorial plane at distances of 2.20-2.60 Å from the U atom. The single water loss intermediate (Supplementary Figure **S1**) can be characterized as $[UO(CAMH_5)]^-$, where one uranyl oxygen was activated and eliminated in the water loss reaction. The U center is coordinated by seven oxygens, with the remaining terminal U=O bond stretched to 1.82 Å and a catechol hydrogen at that same distance from the oxygen. The remaining six oxygens are at an average distance of 2.27 Å from U, with the shortest U-O distance being 2.12 Å. The final product of the double water loss represents a U species in which both uranyl U-O bonds have been activated (Fig. **2**, right panel). Here the U^{6+} center is

coordinated by seven catechol hydrogens with an average U-O bond length of 2.20 Å (shortest is 2.12 Å), all much longer than a typical uranyl double bond. Based on formal charges this species would reflect the presence of a U^{6+} ion normally only found with strong uranyl bonds for organic chelates or in the presence of strong inorganic ligands such as fluorides. Calculated reaction energies for the water loss process show that the overall reaction process requires only 132 kJ/mol, with the first water loss and oxygen activation requiring about 107 kJ/mol, and the second water loss requiring only 25 kJ/mol. This low energy requirement is well within the range of the energy generated during the CID experiments.

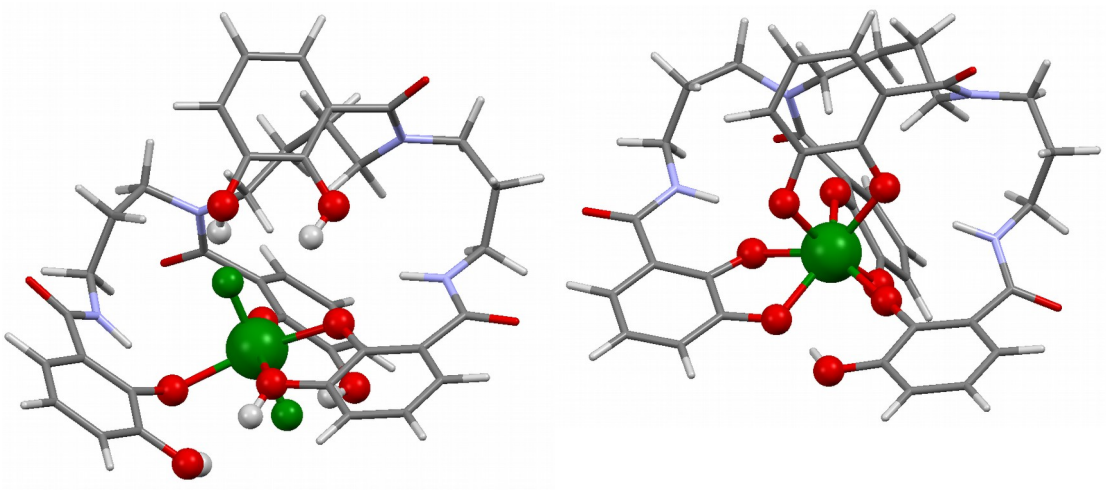

Figure 2. Computed structures of the reactant $[UO_2(CAMH_7)]^-$ (left) and the dehydrated (-$2H_2O$) product $[U(CAMH_3)]^-$ (right). Hydroxyl groups from the catechol binding units are highlighted in ball and stick representation. The "yl" U=O bonds are highlighted in green and a size ratio uranium/oxygen of 1.6 was used for clarity.

The gas-phase double activation of UO_2^{2+} by $CAMH_7^{3-}$ was unambiguously confirmed by IRMPD spectroscopy. Figure **3** shows the IRMPD spectra of the parent fragment $[UO_2(CAMH_7)]^-$, which exhibits an absorbance band at 912 cm^{-1}, characteristic of a ν_3 asymmetric stretching mode of the uranyl double oxo bonds. The calculated spectrum for $[UO_2(CAMH_7)]^-$ shows good agreement, though the two peaks at 860 cm^{-1} and 912 cm^{-1} in the calculated spectrum are computed significantly closer together (~25 cm^{-1} splitting). Analysis of the vibrational modes confirms that the 912 cm^{-1} peak has the uranyl asymmetric stretch as its primary component, and the other two peaks in the 700-950 cm^{-1} are assigned to vibrations of the ligands. The uranyl frequency in this chelate is lower than those of uranyl nitrate (964 cm^{-1}),[29] halide (956-966 cm^{-1}),[30] acetone (988-1017 cm^{-1})[31] and alcohol (944-952 cm^{-1})[32] species previously studied by IRMPD. This red shift is consistent with the higher donation of electron density to the metal center induced by the chelator when compared to weaker donor ligands mentioned above. The IRMPD spectrum of the fragment at m/z = 977 (Fig. **1**) resulting from the loss of two water molecules from the parent ion $[UO_2(CAMH_7)]^-$, clearly shows the disappearance of the uranyl asymmetric stretch IR band at ~912 cm^{-1} (Fig. **3**) indicating the absence of the uranyl moiety in the fragment species.

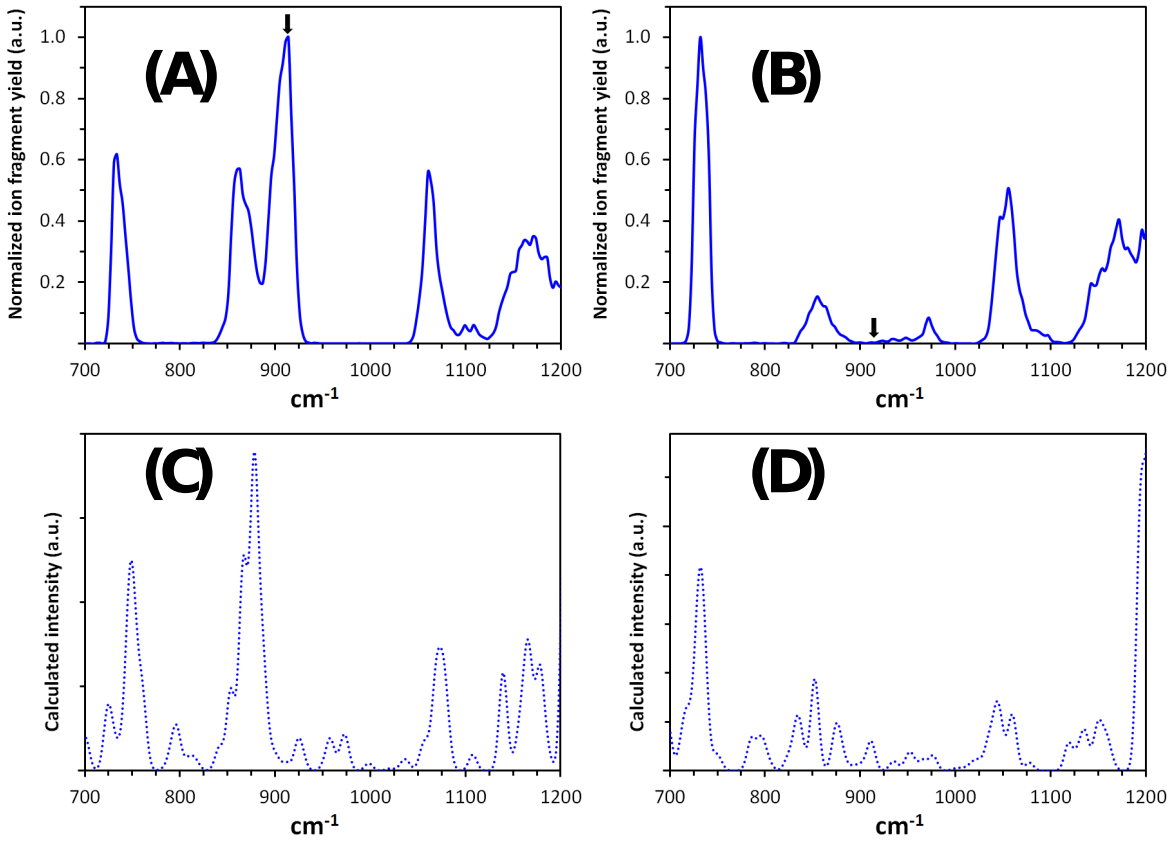

Figure 3. Experimental IRMPD spectra of $[UO_2(CAMH_7)]^-$ (m/z 1013) (A) and its CID fragment resulting from the loss of two H_2O (m/z 977) (B), with corresponding calculated spectra for the parent (C) and fragmented (D) species. Comparison of the spectra shows experimental and predicted disappearance of the uranyl asymmetric stretch mode at ~910 cm^{-1} (indicated with black arrows on experimental spectra) upon loss of two H_2O.

Confirmation of the activation of both uranyl bonds by the $CAMH_7^{3-}$ ligand was obtained with CID ESI-MS experiments using oxygen-18 labeled uranyl, $U^{18}O_2^{2+}$. ESI of a solution of $CAMH_{10}$ and $U^{18}O_2Cl_2$ in ethanol yielded $[U^{18}O_2(CAMH_7)]^-$ (m/z = 1017), as expected from non-labeled

experiments (Fig. **4**). Upon CID, the labeled complex eliminated a fragment of m/z 40 that was attributed to the elimination of two labeled water molecules $H_2{}^{18}O$. This double elimination can only be due to the cleavage of the two U=^{18}O bonds. As observed in the experiments with natural uranyl, the labeled complex also exhibits an alternative dissociation pathway with the elimination of one catecholamide binding unit (m/z = 136) resulting in a fragmented uranyl species of m/z 881, as well as the eliminations of one or two $H_2{}^{18}O$ molecule(s) yielding U complexes of m/z 861 and 841. The final elimination of an ^{16}OH fragment was also observed as in the case of the non-labeled experiments. This fragmentation pattern provides evidence of the complete cleavage of the U=O double bonds with loss of the uranyl O atoms in the uranyl-3,4,3-LI(CAM) system. Combined with computations, the experimental results obtained with natural uranyl-CAM (deuterated and non-deuterated) and with ^{18}O-labeled uranyl-CAM complexes represent the first mechanistic evidence for double activation of UO_2^{2+} by an organic ligand.

In an attempt to extend the results obtained with $CAMH_{10}$, corresponding CID and IRMPD experiments were performed using the ligand 3,4,3-LI(1,2-HOPO) (hereafter designated as $HOPOH_6$), which has the same spermine scaffold as $CAMH_{10}$ but binds metal through four 1-hydroxy-pyridin-2-one (1,2-HOPO) moieties (Fig. **5**).

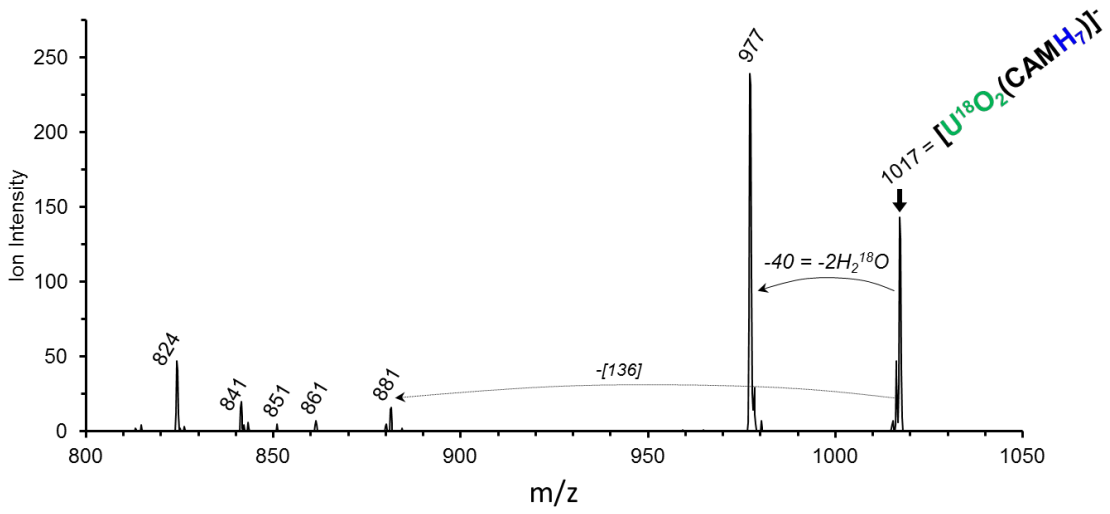

Figure 4. CID mass spectrum of labeled $[U^{18}O_2(CAMH_7)]^-$. Nominal CID voltage = 0.25 V. The dominant pathway is loss of two $H_2{}^{18}O$, indicating elimination of the uranyl oxo-ligands during dehydration. As in Figure 1, a loss of "136" is observed. The peaks at 881, 841, and 824 m/z correspond to the respective losses of "136" and one $H_2{}^{18}O$; "136" and two $H_2{}^{18}O$; "136", two $H_2{}^{18}O$, and one OH from $[U^{18}O_2(CAMH_7)]^-$. Note that the ion intensities are much lower than in Figure 1.

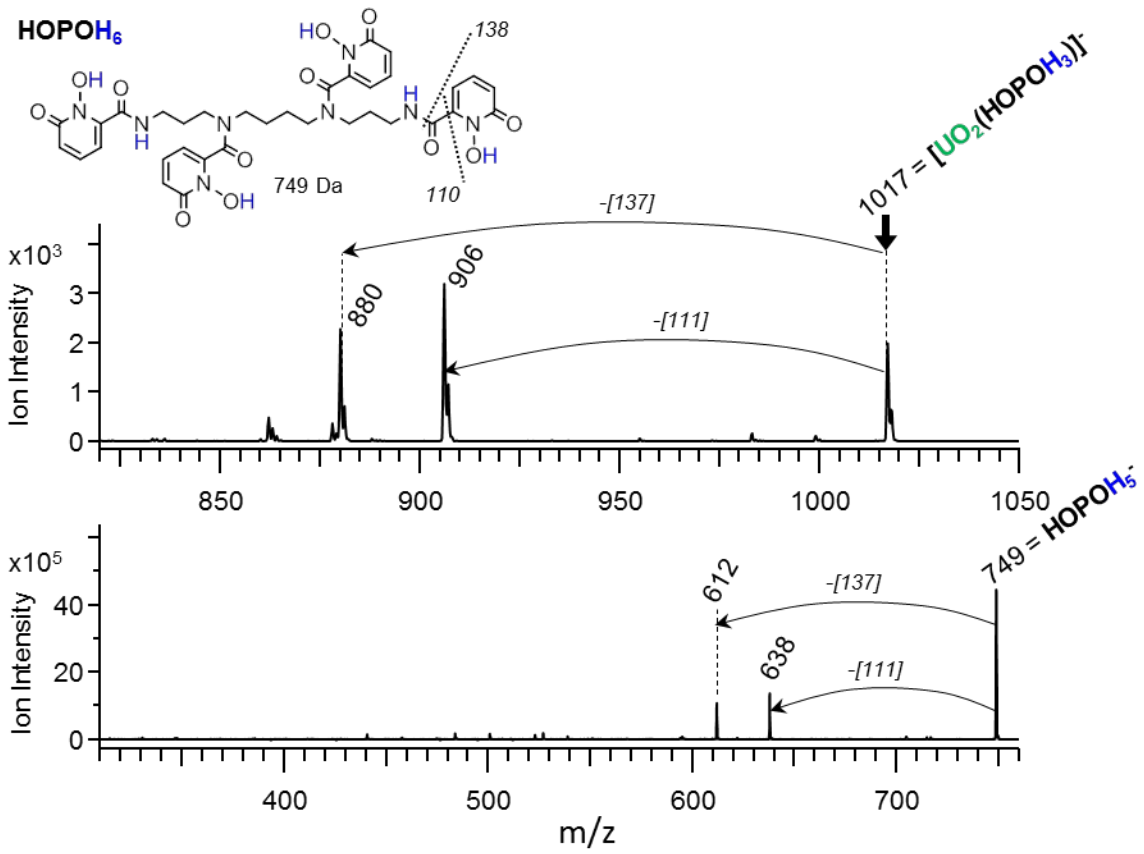

Figure 5. (A) CID ESI-MS spectrum of $[UO_2(HOPOH_3)]^-$. Nominal CID voltage = 0.40 V. (B) CID ESI-MS spectrum of the ligand $HOPOH_6$. Nominal CID voltage = 0.60 V. The dominant fragmentation pathways for both are losses of neutral "111" and "137", which correspond to cleavage of the ligand, as indicated on the structure, with transfer of an H-atom.

This ligand has previously demonstrated a high affinity for UO_2^{2+} in aqueous solutions, and both *in vitro* and *in vivo*.[15,33] Contrasting with $CAMH_{10}$, the ESI-CID mass spectrum of ethanol solutions containing UO_2Cl_2 and $HOPOH_6$ did not yield the elimination of water molecules (Fig. **5**). The observed gas-phase complex produced by ESI, $[UO_2(HOPOH_3)]^-$ (m/z = 1017), exhibited

a distinct uranyl IR stretch (ν_3 = 920 cm^{-1}, Supplementary Figure S2). The result that the ν_3 IR band is much sharper for $[UO_2(HOPOH_3)]^-$ versus $[UO_2(CAMH_7)]^-$ (compare Figs. 3 and S2) suggests that in the HOPO complex the uranyl moiety is not perturbed by hydrogens and may therefore not be activated as it is in the CAM complex. Fragmentation of $[UO_2(HOPOH_3)]^-$ occurred via the cleavage of the C-N secondary amide bond or of the C-C bond linking the 1,2-HOPO group to the secondary amide function. Experiments with and without uranyl present in the $HOPOH_6$ system resulted in the same elimination pathways. The behavior of $[UO_2(HOPOH_3)]^-$ clearly differs from that of $[UO_2(CAMH_7)]^-$, highlighting the specificity of $CAMH_{10}$ toward uranyl binding and activation. Comparison of the CID results obtained with the HOPO- and CAM-uranyl complexes strongly suggests that the breaking of the extremely stable U=O bonds, observed with $CAMH_{10}$, results from interactions between uranyl oxygens and ligand hydroxyl protons of the catechol units, which are not available in the case of $HOPOH_6$.

Conclusions

Double activation of uranyl oxo bonds was achieved through CID fragmentation of the gas-phase $[UO_2(CAMH_7)]^-$ complex. Notably, this non-reductive process resulted in the formation and isolation of a chelated $[U(CAMH_3)]^-$ species comprising a formal U^{6+} metal center coordinated by the organic ligand. The use of a multidentate organic ligand, $CAMH_{10}$, with high affinity for UO_2^{2+} but that still bears hydroxyl protons available for interactions with uranyl oxygens was instrumental, as determined by the lack of reactivity observed with synthetic analog $HOPOH_6$. Although the oxo-bond cleavages are endothermic, the low activation energies calculated for the loss of two water molecules from $[UO_2(CAMH_7)]^-$ suggest a cooperative mechanism between the first and second activation reactions. Further investigations of these reactions with other actinyl ions as well as in condensed phases should determine whether

$CAMH_{10}$ and derivatives may constitute a new class of reagents for actinyl-oxo activation in condensed phases.

ASSOCIATED CONTENT

Supporting Information. Additional computed structures, IRMPD spectra, and Cartesian coordinates for all calculated geometries. This material is available free of charge via the Internet at http://pubs.acs.org

ACKNOWLEDGMENT

This work was supported by the U.S. Department of Energy (DOE), Office of Science, Office of Basic Energy Sciences, Chemical Sciences, Geosciences, and Biosciences Division at the Lawrence Berkeley National Laboratory under Contract DE-AC02-05CH1123 (R.J.A. and J.K.G.), by start-up funds from the Bayer School of Natural and Environmental Sciences and Duquesne University (M.V.S), and by the Netherlands Organisation for Scientific Research under vici-grant no. 724.011.002 and the Stichting Physica (J. O.). It used resources of the Oak Ridge Leadership Computing Facility, a U.S. DOE Office of Science User Facility supported under Contract DE-AC05-00OR22725, and of the National Energy Research Scientific Computing Center (NERSC), which is supported by the Director, Office of Science, Office of Basic Energy Sciences, of the U.S. DOE under Contract No. DE-AC02-05CH11231. The Innovative and Novel Computational Impact on Theory and Experiment (INCITE) program provided an award of computer time.

AUTHOR INFORMATION

Corresponding Authors

* rjabergel@lbl.gov

* wadejong@lbl.gov

* jkgibson@lbl.gov

Notes

The authors declare no competing financial interest.

REFERENCES

(1) Wang, F.; Li, H.; Liu, Q.; Li, Z.; Li, R.; Zhang, H.; Liu, L.; Emelchenko, G.; Wang, J. A Graphene Oxide/Amidoxime Hydrogel for Enhanced Uranium Capture. *Sci. Rep.* **2016**, *6*.

(2) Lu, Y. Uranium Extraction: Coordination Chemistry in the Ocean. *Nat. Chem.* **2014**, *6* (3), 175–177.

(3) Endrizzi, F.; Leggett, C. J.; Rao, L. Scientific Basis for Efficient Extraction of Uranium from Seawater. I: Understanding the Chemical Speciation of Uranium under Seawater Conditions. *Ind. Eng. Chem. Res.* **2016**, *55* (15), 4249–4256.

(4) Moeyaert, P.; Dumas, T.; Guillaumont, D.; Kvashnina, K.; Sorel, C.; Miguirditchian, M.; Moisy, P.; Dufrêche, J.-F. Modeling and Speciation Study of Uranium (VI) and Technetium (VII) Coextraction with DEHiBA. *Inorg. Chem.* **2016**, *55* (13), 6511–6519.

(5) Maloubier, M.; Solari, P. L.; Moisy, P.; Monfort, M.; Den Auwer, C.; Moulin, C. XAS and TRLIF Spectroscopy of Uranium and Neptunium in Seawater. *Dalton Trans.* **2015**, *44* (12), 5417–5427.

(6) Fox, A. R.; Bart, S. C.; Meyer, K.; Cummins, C. C. Towards Uranium Catalysts. *Nature* **2008**, *455* (7211), 341–349.

(7) Arnold, P. L.; Pécharman, A.-F.; Hollis, E.; Yahia, A.; Maron, L.; Parsons, S.; Love, J. B. Uranyl Oxo Activation and Functionalization by Metal Cation Coordination. *Nat. Chem.* **2010**, *2* (12), 1056–1061.

(8) Arnold, P. L.; Pécharman, A.-F.; Lord, R. M.; Jones, G. M.; Hollis, E.; Nichol, G. S.; Maron, L.; Fang, J.; Davin, T.; Love, J. B. Control of Oxo-Group Functionalization and Reduction of the Uranyl Ion. *Inorg. Chem.* **2015**, *54* (7), 3702–3710.

(9) Sarsfield, M. J.; Helliwell, M. Extending the Chemistry of the Uranyl Ion: Lewis Acid Coordination to a UO Oxygen. *J. Am. Chem. Soc.* **2004**, *126* (4), 1036–1037.

(10) Gong, Y.; De Jong, W. A.; Gibson, J. K. Gas Phase Uranyl Activation: Formation of a Uranium Nitrosyl Complex from Uranyl Azide. *J. Am. Chem. Soc.* **2015**, *137* (18), 5911–5915.

(11) Gong, Y.; Vallet, V.; del Carmen Michelini, M.; Rios, D.; Gibson, J. K. Activation of Gas-Phase Uranyl: From an Oxo to a Nitrido Complex. *J. Phys. Chem. A* **2013**, *118* (1), 325–330.

(12) Van Stipdonk, M. J.; Michelini, M. del C.; Plaviak, A.; Martin, D.; Gibson, J. K. Formation of Bare UO22+ and NUO+ by Fragmentation of Gas-Phase Uranyl–Acetonitrile Complexes. *J. Phys. Chem. A* **2014**, *118* (36), 7838–7846.

(13) Leverd, P. C.; Rinaldo, D.; Nierlich, M. Crystal Structure Determination of 4f–5f Heterometallic Complexes. *J. Chem. Soc. Dalton Trans.* **2002**, No. 6, 829–831.

(14) Fortier, S.; Hayton, T. W. Oxo Ligand Functionalization in the Uranyl Ion (UO 2 2+). *Coord. Chem. Rev.* **2010**, *254* (3), 197–214.

(15) Abergel, R. J.; Durbin, P. W.; Kullgren, B.; Ebbe, S. N.; Xu, J.; Chang, P. Y.; Bunin, D. I.; Blakely, E. A.; Bjornstad, K. A.; Rosen, C. J. Biomimetic Actinide Chelators: An Update

on the Preclinical Development of the Orally Active Hydroxypyridonate Decorporation Agents 3, 4, 3-LI (1, 2-HOPO) and 5-LIO (Me-3, 2-HOPO). *Health Phys.* **2010**, *99* (3), 401.

(16) Captain, I.; Deblonde, G. J.-P.; Rupert, P. B.; An, D. D.; Illy, M.-C.; Rostan, E.; Ralston, C. Y.; Strong, R. K.; Abergel, R. J. Engineered Recognition of Tetravalent Zirconium and Thorium by Chelator–Protein Systems: Toward Flexible Radiotherapy and Imaging Platforms. *Inorg. Chem.* **2016**, *55* (22), 11930–11936.

(17) Meinrath, G. Aquatic Chemistry of Uranium. *Geoscience* **1998**, *1* (1), 101.

(18) Gong, Y.; Gibson, J. K. Formation and Characterization of the Uranyl–SO2 Complex, UO2 (CH3SO2)(SO2)−. *J. Phys. Chem. A* **2013**, *117* (4), 783–787.

(19) Rios, D.; Rutkowski, P. X.; Shuh, D. K.; Bray, T. H.; Gibson, J. K.; Van Stipdonk, M. J. Electron Transfer Dissociation of Dipositive Uranyl and Plutonyl Coordination Complexes. *J. Mass Spectrom.* **2011**, *46* (12), 1247–1254.

(20) Rios, D.; Michelini, M. C.; Lucena, A. F.; Marçalo, J.; Bray, T. H.; Gibson, J. K. Gas-Phase Uranyl, Neptunyl, and Plutonyl: Hydration and Oxidation Studied by Experiment and Theory. *Inorg. Chem.* **2012**, *51* (12), 6603–6614.

(21) Oepts, D.; Van der Meer, A.; Van Amersfoort, P. The Free-Electron-Laser User Facility FELIX. *Infrared Phys. Technol.* **1995**, *36* (1), 297–308.

(22) Hu, S.-X.; Gibson, J. K.; Li, W.-L.; Van Stipdonk, M. J.; Martens, J.; Berden, G.; Redlich, B.; Oomens, J.; Li, J. Electronic Structure and Characterization of a Uranyl Di-15-Crown-5 Complex with an Unprecedented Sandwich Structure. *Chem. Commun.* **2016**, *52* (86), 12761–12764.

(23) Dau, P. D.; Rios, D.; Gong, Y.; Michelini, M. C.; Marçalo, J.; Shuh, D. K.; Mogannam, M.; Van Stipdonk, M. J.; Corcovilos, T. A.; Martens, J. K. Synthesis and Hydrolysis of Uranyl, Neptunyl, and Plutonyl Gas-Phase Complexes Exhibiting Discrete Actinide–Carbon Bonds. *Organometallics* **2016**, *35* (9), 1228–1240.

(24) Martens, J.; Berden, G.; Gebhardt, C. R.; Oomens, J. Infrared Ion Spectroscopy in a Modified Quadrupole Ion Trap Mass Spectrometer at the FELIX Free Electron Laser Laboratory. *Rev. Sci. Instrum.* **2016**, *87* (10), 103108.

(25) Martens, J.; Grzetic, J.; Berden, G.; Oomens, J. Structural Identification of Electron Transfer Dissociation Products in Mass Spectrometry Using Infrared Ion Spectroscopy. *Nat. Commun.* **2016**, *7*.

(26) Valiev, M.; Bylaska, E. J.; Govind, N.; Kowalski, K.; Straatsma, T. P.; Van Dam, H. J.; Wang, D.; Nieplocha, J.; Apra, E.; Windus, T. L. NWChem: A Comprehensive and Scalable Open-Source Solution for Large Scale Molecular Simulations. *Comput. Phys. Commun.* **2010**, *181* (9), 1477–1489.

(27) Küchle, W.; Dolg, M.; Stoll, H.; Preuss, H. Energy-adjusted Pseudopotentials for the Actinides. Parameter Sets and Test Calculations for Thorium and Thorium Monoxide. *J. Chem. Phys.* **1994**, *100* (10), 7535–7542.

(28) Godbout, N.; Salahub, D. R.; Andzelm, J.; Wimmer, E. Optimization of Gaussian-Type Basis Sets for Local Spin Density Functional Calculations. Part I. Boron through Neon, Optimization Technique and Validation. *Can. J. Chem.* **1992**, *70* (2), 560–571.

(29) Groenewold, G. S.; Van Stipdonk, M. J.; Oomens, J.; De Jong, W. A.; McIlwain, M. E. The Gas-Phase Bis-Uranyl Nitrate Complex [(UO 2) 2 (NO 3) 5]−: Infrared Spectrum and Structure. *Int. J. Mass Spectrom.* **2011**, *308* (2), 175–180.

(30) Groenewold, G. S.; Van Stipdonk, M. J.; Oomens, J.; De Jong, W. A.; Gresham, G. L.; McIlwain, M. E. Vibrational Spectra of Discrete UO 2 2+ Halide Complexes in the Gas Phase. *Int. J. Mass Spectrom.* **2010**, *297* (1), 67–75.

(31) Groenewold, G. S.; Gianotto, A. K.; Cossel, K. C.; Van Stipdonk, M. J.; Moore, D. T.; Polfer, N.; Oomens, J.; De Jong, W. A.; Visscher, L. Vibrational Spectroscopy of Mass-Selected [UO2 (Ligand) N] 2+ Complexes in the Gas Phase: Comparison with Theory. *J. Am. Chem. Soc.* **2006**, *128* (14), 4802–4813.

(32) Groenewold, G. S.; Van Stipdonk, M. J.; De Jong, W. A.; Oomens, J.; Gresham, G. L.; McIlwain, M. E.; Gao, D.; Siboulet, B.; Visscher, L.; Kullman, M. Infrared Spectroscopy of Dioxouranium (V) Complexes with Solvent Molecules: Effect of Reduction. *ChemPhysChem* **2008**, *9* (9), 1278–1285.

(33) Sturzbecher-Hoehne, M.; Deblonde, G. J.-P.; Abergel, R. J. Solution Thermodynamic Evaluation of Hydroxypyridinonate Chelators 3,4,3-LI(1,2-HOPO) and 5-LIO(Me-3,2-HOPO) for UO2(VI) and Th(IV) Decorporation. *Radiochim. Acta* **2013**, *101* (6), 359–366 DOI: 10.1524/ract.2013.2047.

Table of Content Graphic

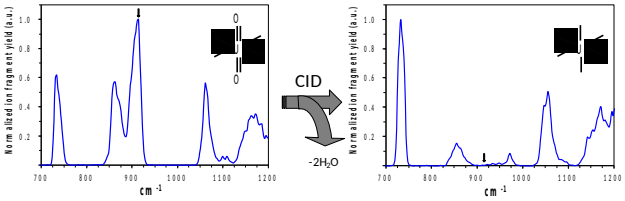

Table of Content Synopsis

Chelate and activate: Non-reductive activation of both uranyl oxo bonds was experimentally evidenced and characterized in the gas phase upon chelation of uranyl by an organic siderophore derivative and subsequent collision induced dissociation. The resulting species is a formal U^{6+} chelate.